CHAPTER 2

Dynamic Soil Properties and Liquefaction

2.1 OVERVIEW

Several problems in engineering practice require knowledge of the dynamic soil properties and liquefaction. Generally, problems related to foundations and retaining structures subjected to dynamic loads problems are divided into either a small strain amplitude or large strain amplitude response. Structures during earthquakes are able to tolerate large strain levels. The major soil properties that are required to analyze the behaviour of a structure subjected to dynamic loads are:

1. Dynamic Young's modulus (E) and dynamic shear modulus (G)
2. Poisson's ratio (μ)
3. Damping usually in terms of damping ratio (ξ)
4. Liquefaction parameters like cyclic shearing stress ratio and cyclic deformation.

Values of E and G are dependent on confining pressure and strain level. There are various tests available for determining E and G. It has been observed that in general Poisson's ratio (μ) varies from 0.25 and 0.35 for cohesionless soils and from about 0.35 and 0.45 for cohesive soils. Responses of structure-foundation-soil systems are not sensitive to the variations in the value of μ. Damping ratio of the medium may be obtained by performing dynamic tests. Methods are available to obtain cyclic stress ratio for examining the liquefaction potential. Discussions on all these aspects have been included in this chapter.

2.2 RESONANT COLUMN TEST

Resonant column test is a laboratory method used as a non-destructive testing technique to obtain the elastic modulus (E), shear modulus (G) and damping characteristics of soils at low strain amplitudes. This test is based on the theory of wave propagation in prismatic rods (Richart, Hall and Woods, 1970). In this test, a column of soil material is excited either longitudinally or torsionally in one of its normal modes and the wave velocity is determined from the frequency at resonance and dimensions of the test sample. The test can be performed with various end conditions of the column; the fixed free end condition is most commonly used (Fig. 2.1).

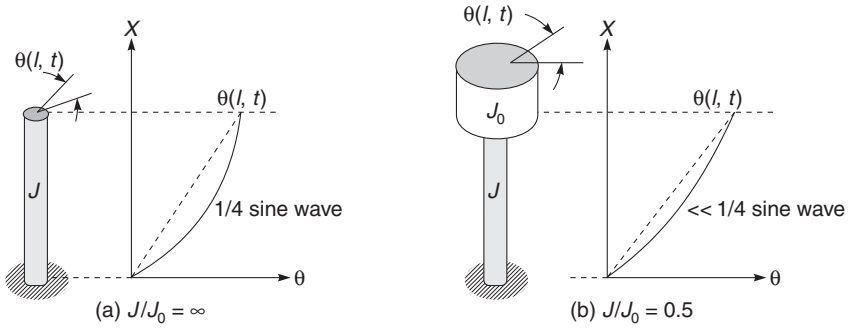

Fig. 2.1 Schematic of resonant column with fixed-free end condition

When the column of the soil is excited longitudinally, compression waves propagate through the specimen. In case the column of the soil is excited torsionally, shear waves propagate. Previously solid samples were used. Recently hollow samples have been used with advantage. In hollow specimen, the variation in shearing strain across the thickness of the cylinder wall becomes relatively small (Drnewich, 1967, 1972; Anderson, 1974; Woods, 1978). The modulus is determined from the resonant frequency and geometric properties of the specimen and the driving apparatus. Damping is determined by switching off the driving power at resonance and recording the amplitude of the decaying vibrations from which the logarithmic decrement is calculated. Damping ratio may also be obtained from frequency response curve using the bandwidth method. Figure 2.2 shows a sketch of hollow specimen resonant column apparatus.

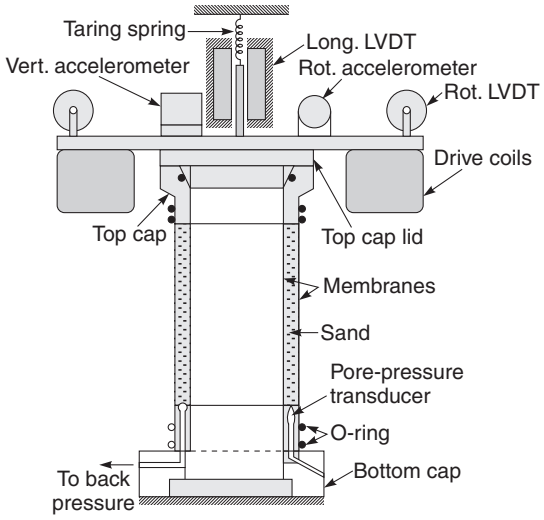

Fig. 2.2 Hollow specimen resonant column apparatus (Drnevich, 1972)

For a fixed-free column subjected to longitudinal vibrations in the first normal mode, the velocity of the longitudinal wave, V_l, is given by:

$$\frac{W}{W_o} = \frac{\omega_{nl} h}{V_l} \tan\left(\frac{\omega_{nl} h}{V_l}\right) \quad ...(2.1)$$

where,

W = weight of specimen,

W_o = weight of loading system,

ω_{nl} = natural frequency of first natural mode, and

h = height of the specimen.

If the loading system is massless (i.e., $W_o = 0$), Eq. (2.1) reduces to;

$$V_l = \frac{2\omega_{nl} h}{\pi} \quad ...(2.2a)$$

or,

$$V_l = 4 f_{nl} h \quad ...(2.2b)$$

f_{nl} is the natural frequency in cps.

Knowing the value of V_l, value of dynamic Young's modulus (E) is obtained by:

$$E = \rho V_l^2 \quad ...(2.3)$$

where,

ρ = mass density of soil specimen.

For solid specimen,

$$\rho = \frac{4W}{\pi d^2 hg} = \frac{\gamma}{g} \quad ...(2.4a)$$

For hollow specimen,

$$\rho = \frac{4W}{\pi(d_o^2 - d_i^2)\ hg} = \frac{\gamma}{g} \quad ...(2.4b)$$

where,

W = total weight of specimen,

d = diameter of solid specimen,

d_o = outer diameter of hollow specimen,

d_i = inner diameter of hollow specimen,

g = acceleration due to gravity, and

γ = unit weight of soil at which specimen is prepared.

If the fixed-free column is excited torsionally, the shear wave velocity (V_s) is given by:

$$\frac{I}{I_o} = \frac{\omega_{ns} h}{V_s} \tan\left(\frac{\omega_{ns} h}{V_s}\right) \quad ...(2.5)$$

where,

I = mass polar moment of inertial of the specimen, and

I_o = mass polar moment of inertial of the torsional loading system connected to the top of the specimen.

If the loading system is massless (i.e., $I_o = 0$), Eq. (2.5) reduces to:

$$V_s = \frac{2\omega_{ns} h}{\pi} \qquad ...(2.6a)$$

or, $$V_s = 4 f_{ns} h \qquad ...(2.6b)$$

Knowing the value of V_s, value of dynamic shear modulus (G) is obtained by:

$$G = \rho V_s^2 \qquad ...(2.7)$$

Knowing the values of E and G, Poisson's ratio (μ) may be obtained using the following relation,

$$G = \frac{E}{2(1 + \mu)} \qquad ...(2.8a)$$

or, $$\mu = \frac{E}{2G} - 1 \qquad ...(2.8b)$$

2.3 CYCLIC PLATE LOAD TEST

The cyclic plate load test is a modified version of the standard plate load test. This test facilitates in separating the elastic (recoverable) part of deformation from the total settlement which in turn is related to the Young's modulus of the soil.

The cyclic plate load test is performed in a test pit dug upto the proposed base level of foundation. The equipment is same as used in conventional plate load test. Circular or square bearing plates of mild steel not less than 25 mm thickness and varying in size from 300 to 750 mm with chequered or grooved bottom are used. The test pit should be at least five times the width of the plate. The equipment is assembled according to the details given in IS 1988-1982. A typical set-up is shown in Fig. 2.3.

To commence the test, a seating pressure of about 7 kPa is first applied to the plate. It is then removed, dial gauges are set to read zero. Load is then applied in equal cumulative increments of not more than 100 kPa or of not more than one-fifth of the load corresponding to estimated allowable bearing pressure. In cyclic plate load test, each incremental load is maintained constant till the settlement of the plate is complete. The load is then released to zero and the plate is allowed to rebound. The reading of final settlement is taken. The load is then increased to next higher magnitude of loading and maintained constant till the settlement is complete, which again is recorded. The load is then reduced to zero and the settlement reading taken. The next increment of load is then applied. The cycles of unloading and reloading are continued till the required final load is reached.

The data obtained from a cyclic plate load test is shown in Fig. 2.4(a). From this data, the load intensity versus elastic rebound is plotted as shown in Fig. 2.4(b), and the slope of the line is coefficient of elastic uniform compression.

$$C_u = \frac{p}{S_e} \text{ (kN/m}^3\text{)} \qquad ...(2.9)$$

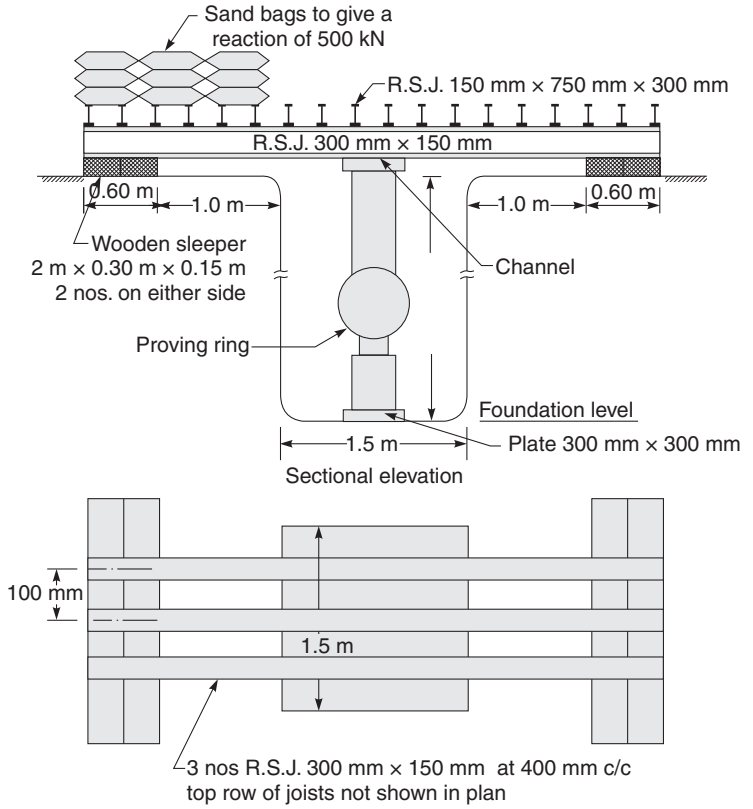

Fig. 2.3 A typical set-up for cyclic plate load test

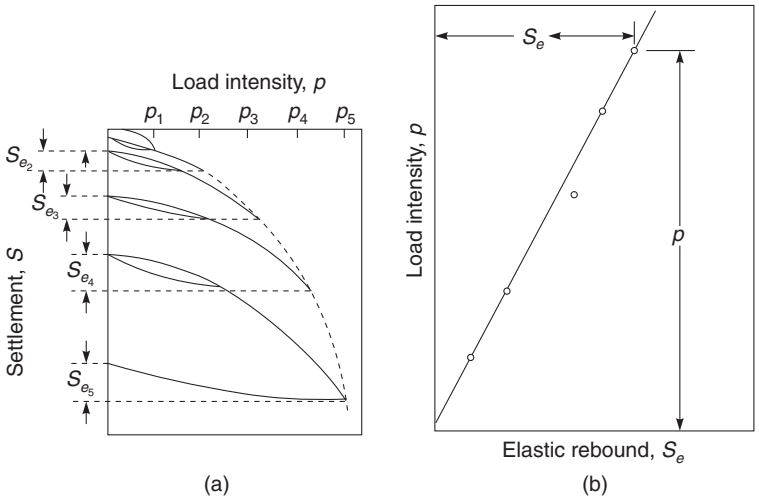

Fig. 2.4 (a) Load intensity versus settlement curve in a cyclic plate load test, (b) Load intensity versus elastic rebound plot from cyclic plate load test

where,

p = load intensity in kN/m^2, and

S_e = elastic rebound corresponding to p in m.

For a square rigid plate of area A in m^2, on an elastic medium subjected to vertical load, C_u is related with E by the relation given below:

$$C_u = \frac{1.08\ E}{(1 - \mu^2)} \frac{1}{\sqrt{A}} \qquad ...(2.10)$$

Value of shear modulus G may be obtained using relation (2.8a) once the value of E is determined using (2.10).

2.4 VERTICAL BLOCK RESONANCE TEST

The vertical block resonance test is used for determining the coefficient of elastic uniform compression (C_u), Young's modulus (E) and damping ratio (ξ_z) of the soil.

According to IS 5249: 1984, a test block of size 1.5 m × 0.75 m × 0.75 m high is cast in M25 concrete in a pit of plan dimensions 4.5 m × 2.75 m and depth equal to the proposed depth of foundation. Foundation bolts should be embedded into the concrete block at the time of casting for fixing the oscillator assembly. The oscillator assembly is mounted on the block so that it generates purely vertical sinusoidal vibrations. The line of action of vibrating force should pass through the centre of gravity of the block. Two acceleration or displacement pickups are mounted on the top of the block as shown in Fig. 2.5 such that they sense the vertical motion of the block. A schematic diagram of the set-up is shown in Fig. 2.5.

The mechanical oscillator works on the principle of eccentric masses each of magnitude m_e mounted on two shafts rotating in opposite directions with speed ω (Fig. 2.6). The force generated by the oscillator is given by

$$F_d = 2m_e e\omega^2 \qquad ...(2.11a)$$

e is the eccentricity given by:

$$e = r \sin(\theta/2) \qquad ...(2.11b)$$

where,

r = crank radius, and

θ = angle between the eccentric masses in degrees.

In a particular oscillator, m_e and r are fixed. Therefore the force generated will depend on the value of θ and its maximum value will be when θ = 180°. In mechanical oscillator, it is convenient to vary θ.

The oscillator is first set at a particular θ°. As evident from Eq. (2.11a) higher the eccentricity more will be the force level. It is then operated at constant frequency, and the acceleration of the oscillatory motion of the block is monitored. The oscillator frequency is increased in steps, and the signals of monitoring pickups are recorded. At any eccentricity and frequency

force level) is different because different forces cause different strain levels of the block which may be accounted for when appropriate design parameters are being chosen.

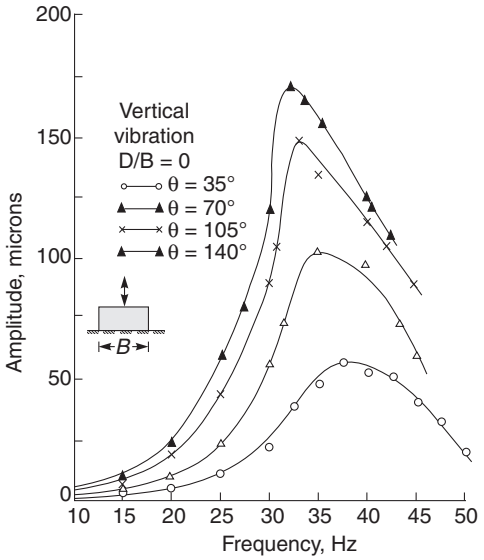

Fig. 2.7 Amplitude versus frequency curves from vertical block resonance test

The coefficient of elastic uniform compression (C_u) in N/m^3 of the soil is then determined using Eq. (2.13)

$$C_u = \frac{4\pi^2 f_{nz}^2 m}{A} \qquad ...(2.13)$$

where,

f_{nz} = natural frequency of foundation-soil system, Hz,

m = mass of the block oscillator and motor, kg, and

A = base contact area of the block, m^2.

The damping ratio may be obtained by bandwidth method. According to this:

$$\xi_z = \frac{f_2 - f_1}{2f_n} \qquad ...(2.14)$$

where, f_1 and f_2 are frequencies at which the amplitude is $1/\sqrt{2}$ times the peak amplitude (Fig. 2.8).

2.5 CROSS BOREHOLE TEST

The cross borehole shear wave method is recommended for shear wave velocity determination because it provides greater measurement accuracy as the observed shear wave travels through a particular strata with less interference from nearby refracting horizons. This method is capable

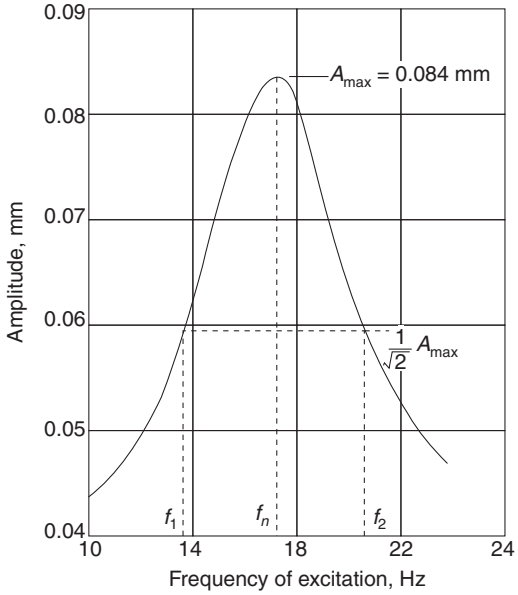

Fig. 2.8 Determination of viscous damping in forced vibrations by bandwidth method

of measuring the dynamic material parameters of individual strata in the soil/rock deposit using horizontally travelling shear waves which can be generated and received at specific depths.

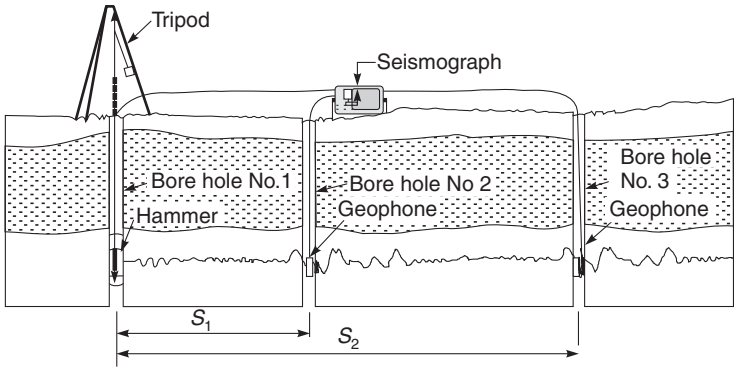

Fig. 2.9 Schematic diagram for cross borehole test

Three vertical boreholes, at known distance apart, are bored to the same depth and cased. A Bison borehole hammer is now lowered into the first borehole (borehole No.1). This is a special type of hammer with hydraulically operated shoes that can be extended or retracted within the borehole as desired. At a predetermined depth, say 2 m, the hammer shoes are hydraulically extended to grip the borehole walls and lock the hammer in place. Now borehole geophones are lowered into the other two boreholes (boreholes No. 2 and 3). These geophones can be locked in the boreholes at any desired depth, 2 m in this case, by the help of specially fitted

rubber bladders, which can be inflated pneumatically. The electrical signals from the borehole hammer and geophones are fed into a Bison seismograph. A schematic diagram for the cross borehole test is shown in Fig. 2.9.

Having locked the borehole hammer and geophones at the same desired depth, 2 m in this case, the seismograph is switched on. A shear wave is now generated in the first borehole by operating the hammer. This activates a timer switch in the seismograph and the shear waveform arrivals at the borehole geophones are displayed on the video screen of the seismograph. The waveforms are now analyzed and the exact arrival time of the shear waves are calculated, for the borehole locations (boreholes no. 2 and 3) and depth (2 m in this case).

The hydraulically operated hammer shoes are now retracted and the hammer lowered to its next depth say 4 m, and again locked in position by extending the shoes. Similarly, the borehole geophones are now lowered and locked at the same new depth of 4 m by deflating and then again inflating the rubber bladders. The shear wave is now generated and the arrival times computed as discussed above for the 2 m depth case.

This process is repeated for as many depths as planned to obtain a shear wave profile for the location under consideration.

Having obtained the shear wave travel time, T_{s1} and T_{s2}, for the known distances between the boreholes (S_1 and S_2, Fig. 2.9), the shear wave velocity (V_s) for a particular depth was obtained as:

$$V_s = S_1/T_{s1} = S_2/T_{s2} \qquad ...(2.14a)$$

Specifications for the Tests

(a) A set of 3 boreholes laid out along a line are needed at each location. The spacing between the boreholes depends on the data of borelogs from the site. The boreholes should be cleaned and cased with PVC casing pipes and should have an internal diameter of 85 mm to 90 mm. The PVC casing pipes should be able to withstand pressures upto 1000 kN/m^2 (IS 4568 PVC pipes). The cased boreholes should be made upto the required depth.

(b) The boreholes need to be plugged at the bottom and the water inside the cased borehole pumped out.

(c) It is required to have the boreholes made of the same diameter as the PVC casing pipes. In case boreholes of 150 mm diameter are first made and then the PVC casings of 85 mm to 90 mm internal diameter are installed in them, the annular space between the 150 mm diameter hole and the PVC casing is to be backfilled with a clean sand slurry. The backfilling has to be done properly as if there are any voids this will affect the resultant shear wave velocity. The shear wave cannot travel through voids.

2.6 SASW TEST

The Spectral Analysis of Surface Waves (SASW) is a new seismic method for quick and economical determination of shear wave velocity (*in situ*). It utilizes the dispersive nature

where,

S = shear strength of sand,

$\overline{\sigma}_n$ = effective normal pressure on any plane xx at depth z

= $\gamma\, h_w + \gamma_{sub}\, (Z - h_w)$,

ϕ = angle of internal friction,

γ = unit weight of soil above water table, and

γ_{sub} = submerged unit weight of soil.

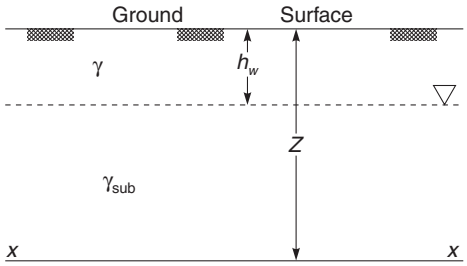

Fig. 2.11 Section of ground showing the position of water table

If a saturated sand is subjected to ground vibrations, it tends to compact and decrease in volume, if drainage is restrained the tendency to decrease in volume results in an increase in pore pressure. The strength may now be expressed as,

$$S_{dyn} = (\overline{\sigma}_n - u_{dyn}) \tan \phi_{dyn} \qquad ...(2.16)$$

where,

S_{dyn} = shear strength of soil under vibrations,

u_{dyn} = excess pore water pressure due to ground vibrations, and

ϕ_{dyn} = angle of internal friction under dynamic conditions.

It is seen that with development of additional positive pore pressure, the strength of sand is reduced. In sands, ϕ_{dyn} is almost equal to ϕ, i.e., angle of internal friction in static conditions.

For complete loss of strength i.e., S_{dyn} is zero.

Thus, $\overline{\sigma}_n - u_{dyn} = 0$

or, $\overline{\sigma}_n = u_{dyn}$

or, $$\frac{\overline{\sigma}_n}{u_{dyn}} = 1 \qquad ...(2.17)$$

Expressing u_{dyn} in terms of rise in water head, h_w and γ_{sub} as $(G - 1/1 + e)\, \gamma_w$ the Eq. (2.17) can written as:

$$\frac{\gamma_w . h_w}{\dfrac{G - 1}{1 + e}\, \gamma_w Z} = 1$$

or,

$$\frac{h_w}{Z} = \frac{G-1}{1+e} = i_{cr} \qquad ...(2.18)$$

where,

G = specific gravity of soil particles,

e = void ratio, and

i_{cr} = critical hydraulic gradient.

It is seen that, because of increase in pore water pressure the effective stress reduces, resulting in loss of strength. Transfer of intergranular stress takes place from soil grains to pore water. Thus, if this transfer is complete, there is complete loss of strength, resulting in what is known as complete liquefaction. However, if only partial transfer of stress from the grains to the pore water occurs, there is partial loss of strength resulting in partial liquefaction.

In case of complete liquefaction, the effective stress is lost and the sand-water mixture behaves as a viscous material and the process of consolidation starts, followed by surface settlement, resulting in closer packing of sand grains. Thus, the structures resting on such a material start sinking. The rate of sinking of structures depends upon the time for which the sand remains in liquefied state.

Liquefaction of sand may develop at any zone of a deposit, where the necessary combination of *in situ* density, surcharge conditions and vibration characteristics occur. Such a zone may be at the surface or at some depth below the ground surface, depending only on the state of sand and the induced motion.

However, liquefaction of the upper layers of a deposit may also occur, not as a direct result of the ground motion to which they are subjected, but because of the development of liquefaction in an underlying zone of the deposit. Once liquefaction develops at some depth in a mass of sand, the excess pore water pressure in the liquefied zone will dissipate by flow of water in an upward direction. If the hydraulic gradient becomes sufficiently large, the upward flow of water will induce a quick or liquefied condition in the surface layers of the deposit.

Thus, an important feature of the phenomenon of liquefaction is the fact that, its onset in one zone of deposit may lead to liquefaction of other zones, which would have remained stable otherwise.

2.7.3 Factors Affecting Liquefaction

The factors affecting liquefaction are summarized below:

(i) Soil type

Liquefaction occurs in cohesionless soils as they lose their strength completely under vibration due to the development of pore pressures which in turn reduce the effective stress to zero. Liquefaction does not occur in case of cohesive soils. Only highly sensitive clays may lose their strength substantially under vibration.

(vii) Method of soil formation

Sands unlike clays do not exhibit a characteristic structure. But recent investigations show that liquefaction characteristics of saturated sands under cyclic loading are significantly influenced by the method of sample preparation and by soil structure.

(viii) Period under sustained load

Age of sand deposit may influence its liquefaction characteristics. A 75% increase in liquefaction resistance has been reported on liquefaction of undisturbed sand compared to its freshly prepared sample which may be due to some form of cementation or welding at contact points of sand particles and associated with secondary compression of soil.

(ix) Previous strain history

Studies on liquefaction characteristics of freshly deposited sand and of similar deposit previously subjected to some strain history reveal, that although the prior strain history caused no significant change in the density of the sand, it increased the stress that causes liquefaction by a factor of 1.5.

(x) Trapped air

If air is trapped in saturated soil and pore pressure develops, a part of it is dissipated due to the compression of air. Hence, trapped air helps to reduce the possibility to liquefaction.

2.7.4 Evaluation of Zone of Liquefaction

(i) Using cyclic stress ratio method

For evaluation of liquefaction potential, Seed and Idriss (1971) developed standard curves between cyclic resistance ratio ($\sigma_d/2\sigma_3$) versus mean grain size (D_{50}) for 10 to 30 numbers of cycles of stress application for an initial relative density of compaction of 50% (Figs. 2.12 a and b). These curves were prepared by compiling the results of various tests conducted by several investigators on various types of sand.

The values of cyclic resistance ratio ($\tau_h/\overline{\sigma}_v$) causing liquefaction, estimated from the results of simple shear tests, have shown that the value of $\tau_h/\overline{\sigma}_v$ is less than the corresponding value of $\sigma_d/2\sigma_3$ (Figs. 2.12 a and b). The two resistance ratio may be expressed by the following relation:

$$\left(\frac{\tau_h}{\sigma_v}\right)_{\text{field } D_r} = \left(\frac{\sigma_d}{2\sigma_3}\right)_{\text{triax } 50} C_r \frac{D_r}{50} \qquad \text{...(2.19)}$$

where,

D_R = relative density (%), and

C_r = correction factor.

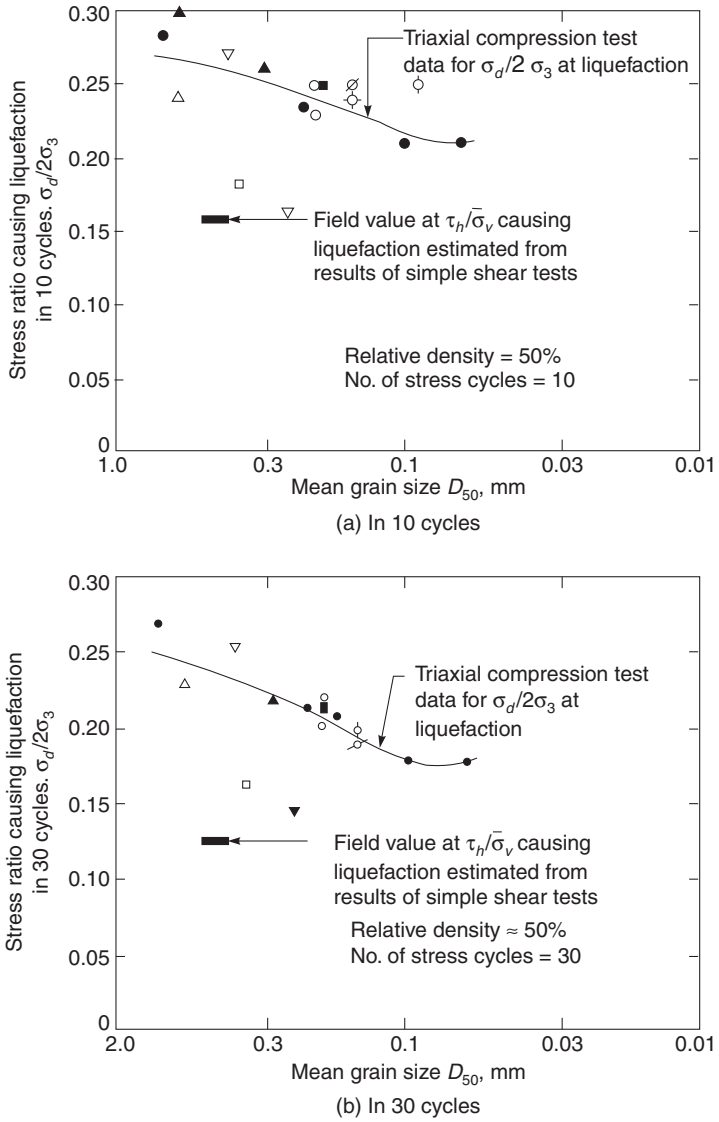

Fig. 2.12 Stress conditions causing liquefaction of sands

Seed and Idriss (1971) suggested the values of C_r as given in Table 2.1.

Table 2.1 Values of C_r

Relative density D_R (%)	C_r	*Remarks*
0 – 50	0.57	Interpolation may be done for intermediate values of D_R
60	0.60	
80	0.68	

Sand compacted at a relative density more than 80% require very huge value of cyclic stress ratio for causing liquefaction.

At a depth below the ground surface, liquefaction will occur if the shear stress induced by an earthquake is more than the shear resistance predicted by Eq. (2.19). By comparing the induced shear stresses and predicted shear resistances at various depths, liquefaction zone can be obtained.

In a sand deposit consider a column of soil of height h and unit area of cross-section subjected to maximum ground acceleration a_{max} (Fig. 2.13). Assuming the soil column to behave as a rigid body, the maximum shear stress τ_{max} at a depth h is given by

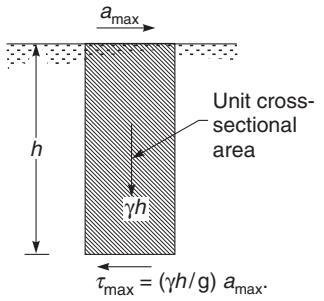

Fig. 2.13 Maximum shear stress at a depth for a rigid soil column

$$\tau_{max} = \left(\frac{\gamma h}{g}\right) a_{max} \qquad ...(2.20)$$

where,

g = acceleration due to gravity, and

γ = unit weight of soil.

Since the soil column behaves as a deformable body, the actual shear stress at depth h, $(\tau_{max})_{act}$ is taken as

$$(\tau_{max})_{act} = r_d \cdot \tau_{max} = r_d \left(\frac{\gamma h}{g}\right) a_{max} \qquad ...(2.21)$$

where, r_d = stress reduction factor.

Seed and Idriss (1971) recommended the use of charts shown in Fig. 2.14 for obtaining the values of r_d at various depths. In this figure the range of r_d for different soil profiles alongwith the average value upto depth of 12 m is shown. The critical depth for development of liquefaction is usually less than 12 m.

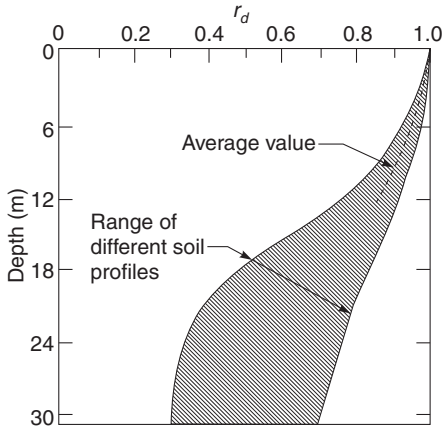

Fig. 2.14 Reduction factor r_d versus depths (Seed and Idriss, 1971)

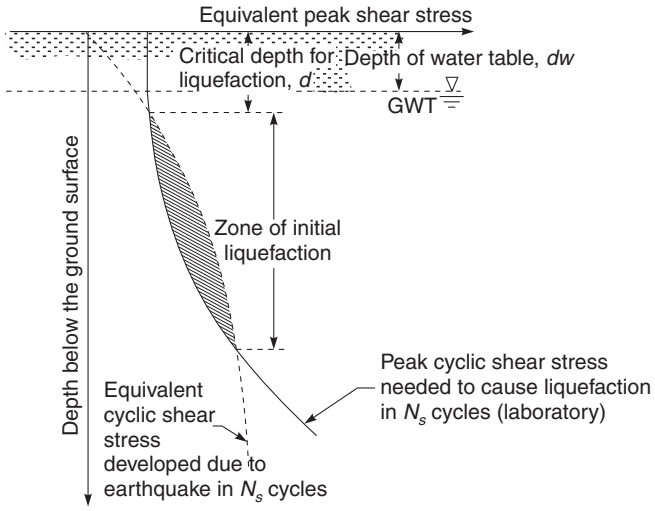

Fig. 2.15 Zone of initial liquefaction in field

where,

N_1 = corrected value of standard penetration resistance, and

C_N = correction factor (Fig. 2.16).

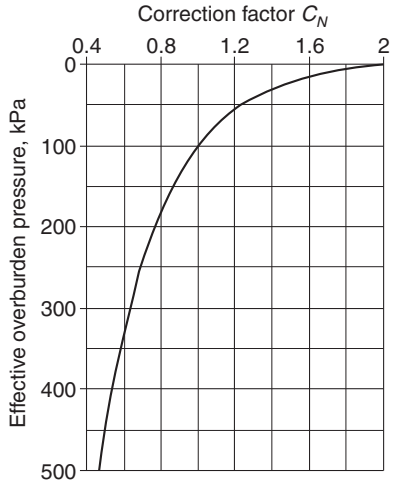

Fig. 2.16 Chart for correction of *N*-values in sand for influence of overburden pressure (Peck et al., 1974)

The correlation between N_1 values and relative density of granular soils suggested by Terzaghi and Peck (1967) is given in Table 2.3.

Table 2.3 N_1 and φ related to relative density

N_1	Compactness	Relative density D_r (%)	φ (Deg)
0-4	Very loose	0-15	< 28
4-10	Loose	15-35	28-30
10-30	Medium	35-65	30-36
30-50	Dense	65-85	36-41
> 50	Very dense	> 85	> 41

After the occurrence of Niigata earthquake, Kishida (1966), Kuizumi (1966), and Ohasaki (1966) studied the areas in Niigata where liquefaction had not occurred and developed criteria for differentiating between liquefaction and non-liquefaction conditions in that city, based on *N*-values of the sand deposits (Seed, 1979). The results of these studies for Niigata are shown in Fig. 2.17. Ohasaki (1970) gave a useful rule of thumb that says liquefaction is not a problem if the blow count from a standard penetration test exceeds twice the depth in metres.

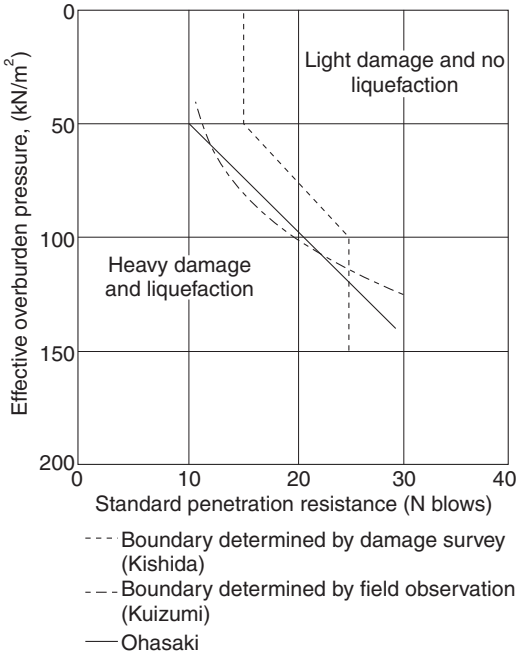

Fig. 2.17 Analysis of liquefaction potential at Niigata for earthquake of June 16, 1994 (Seed, 1979)

On the basis of more comprehensive study on the subject and data presented by other investigators (Seed and Peacock, 1971; Christian and Swiger, 1976; Seed, Mori et al., 1977), Seed (1979) proposed the following procedure for liquefaction analysis:

1. Establish the design earthquake, and obtain the peak ground acceleration a_{max}. Also obtain number of significant cycles corresponding to the magnitude of earthquake using Table 2.2.

2. Using Eq. 2.22, determine τ_{av} at depth h below ground surface.
3. Determine the value of standard penetration resistance value (N) at depth h below ground surface. Obtain corrected N_1 value after applying overburden correction to N using Fig. 2.16.
4. Using Fig. 2.18, determine $(\tau_h/\overline{\sigma}_v)$ for the given magnitude of earthquake and N_1 value obtained in step (iii). Multiplying $(\tau_h/\overline{\sigma}_v)$ with effective stress at depth h below the ground surface, one can obtain the value of shear stress τ_h required for causing liquefaction.

   At depth h, liquefaction will occur if

   $$\tau_{av} > \tau_h$$

   Repeat steps (ii) to (v) for other values of h to locate the zone of liquefaction.

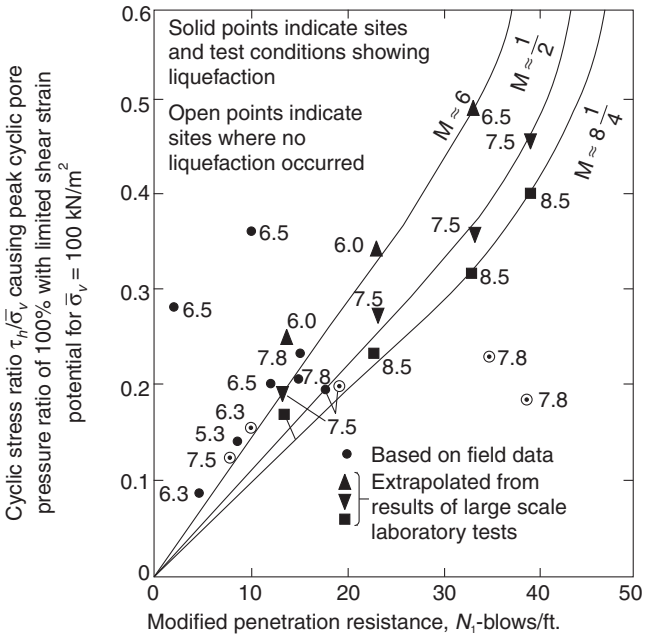

Fig. 2.18 Correlation between field liquefaction behaviour of sand for level ground conditions and penetration resistance (Seed, 1979)

(iii) Evaluation of liquefaction potential using Iwasaki (1986) method

Iwasaki (1986) introduced the concept of liquefaction resistance factor F_L which is defined as

$$F_L = \frac{R}{L} \qquad ...(2.24)$$

R is the ratio of *in situ* cyclic strength of soil and effective overburden pressure. It depends on relative density, effective overburden pressure and mean particle size. It is given by

For $0.02 < D_{50} < 0.6$ mm

$$R = 0.882 \sqrt{\frac{N}{\overline{\sigma}_v + 70}} + 0.225 \log_{10} \left(\frac{0.35}{D_{50}}\right) \quad ...(2.25)$$

For $0.6 < D_{50} < 2.0$ mm

$$R = 0.882 \sqrt{\frac{N}{\overline{\sigma}_v + 70}} - 0.05 \quad ...(2.26)$$

where,

N = observed value of standard penetration resistance,

$\overline{\sigma}_v$ = effective overburden pressure at the depth under consideration for liquefaction examination in kN/m^2,

D_{50} = mean grain size in mm, and

L = ratio of dynamic load induced by seismic motion and effective overburden pressure. It is given by

$$L = \frac{a_{\max}}{g} \frac{\sigma_v}{\overline{\sigma}_v} r_d \quad ...(2.27)$$

$a_{\max}$ = peak ground acceleration due to earthquake

$$= 0.184 \times 10^{0.320M} (D)^{-0.8} \quad ...(2.28)$$

where,

M = magnitude of earthquake on Richter's scale,

D = maximum epicentral distance in km (Fig. 2.19),

σ_v = total overburden pressure,

$\overline{\sigma}_v$ = effective overburden preesure,

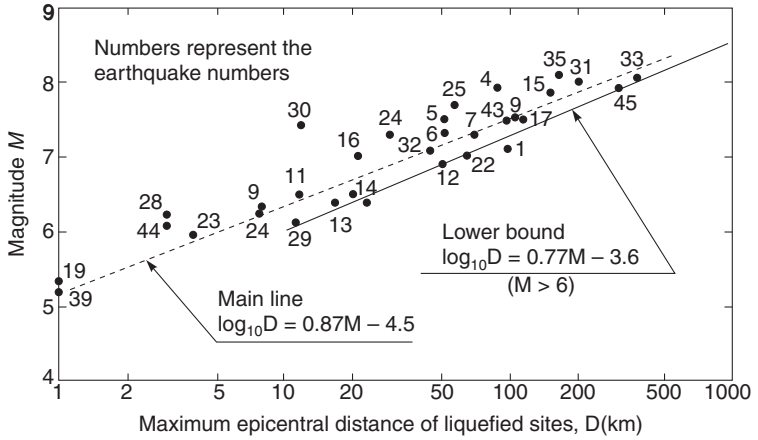

Fig. 2.19 Relationship between the maximum epicentral distance of liquefied site (D) and earthquake magnitude (M) (Kuribayashi, Tatsuoka and Yoshida, 1977)

r_d = reduction factor to account the flexibility of the ground
= 1 – 0.015 h,
g = acceleration due to gravity, m/s^2, and
h = depth of plane below ground surface in m.

For the soil not to liquefy F_L should be greater than unity.

(iv) Evaluation of probability of initiation of liquefaction

Cetin et al. (2004) presented new correlations for obtaining probability of initiation of liquefaction at any depth '*h*' below the ground surface. These new correlations eliminate several sources of bias intrinsic to previous, similar correlations, and provide greatly reduced overall uncertainty and variance. Key elements in the development of these new correlations are: (i) accumulation of a significantly expanded database of field performance case histories; (ii) use of improved knowledge and understanding of factors affecting interpretation of standard penetration test data; (iii) incorporation of improved understanding of factors affecting site-specific earthquake ground motions (including directivity effects, site-specific response, etc.); (iv) use of improved methods for assessment of *in situ* cyclic shear stress ratio; (v) screening of field data case histories on a quality/uncertainty basis; and (vi) use of high-order probabilistic tools (Bayesian updating). The resulting relationships not only provide greatly reduced uncertainty, they also help to resolve a number of corollary issues that have long been difficult and controversial including: (i) magnitude-correlated duration weighting factors, (ii) adjustments for fines content, and (iii) corrections for overburden stress.

The procedure given by Cetin et al. (2004), for obtaining the probability of initiating liquefaction at any depth below the ground surface, can be summarized in the following steps:

1. Obtain the value of standard penetration resistance (N) at the depth h below the ground surface. Correct it for overburden effect using Eq. (2.29)

where,

$$N_1 = N\, C_N \qquad ...(2.29)$$

$$C_N = (100/\sigma'_v)^{0.5} \text{ (Liao and Whiteman, 1986)} \qquad ...(2.30)$$

σ'_v = effective overburden stress at depth h in kN/m^2

If the value of C_N works out more than 1.6 adopt C_N = 1.6.

The resulting N_1 value is further corrected for energy, equipment and procedural effects to obtain fully standardized $N_{1,60}$ value as:

$$N_{1,60} = N_1.\ C_R.C_S.C_B.C_E \qquad ...(2.31)$$

where,

C_R = correction for short rod length,
C_S = correction for non-standardized sample configuration,
C_B = correction for borehole diameter, and
C_E = correction for hammer energy efficiency.

C_R may be obtained using Fig. 2.20.

2. Obtain equivalent cyclic stress ratio (CSR_{Eq}) using the following relation:

$$CSR_{Eq} = 0.65 \left(\frac{a_{max}}{g}\right) \left(\frac{\sigma_v}{\sigma'_v}\right) r_d \quad ...(2.36)$$

where,

a_{max} = peak horizontal ground acceleration,

g = acceleration due to gravity,

σ_v = total vertical stress at depth h,

σ'_v = effective vertical stress at depth h, and

r_d = non-linear shear mass participation factor (Fig. 2.21) (Mayfield et al., 2010).

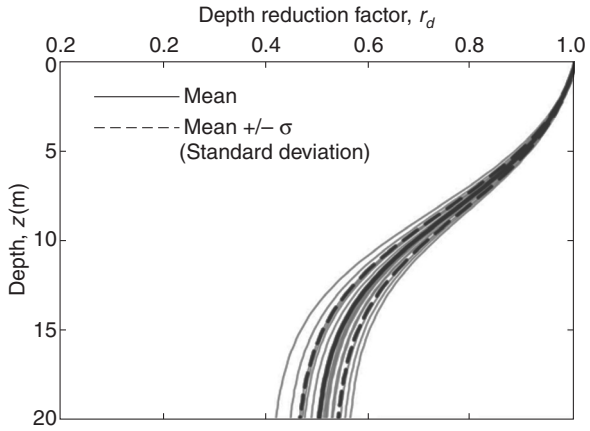

Fig. 2.21 Computed mean r_d profiles with v_s,12 = 175 m/ s for 475-year and 2,475-year peak acceleration and mean magnitude for Butte, Mont.; Charleston, S.C., Eureka, Calif.; Memphis, Tenn.; Portland, Ore.; Salt Lake City; San Francisco; San Jose, Calif.; Santa Monica, Calif.; and Seattle (after Cetin, 2004).

3. Obtain $CSR_{Eq,\ M = 7.5}$ which represents the equivalent CSR_{Eq} for a duration typical of an average equal of magnitude of earthquake (Mw) equal to 7.5, using the following relation:

$$CSR_{Eq,\ M = 7.5} = \frac{CSR_{Eq}}{DWF_M} \quad ...(2.37)$$

where, DWF_M is duration weighting factor and is obtained using Fig. 2.22.

4. Convert the value of $CSR_{Eq,\ M = 7.5}$ corresponding to 1 atmosphere pressure using the following relation:

$$CSR_{Eq,\ M = 7.5,\ 1\ at} = \frac{CSR_{Eq,\ M = 7.5}}{K_\sigma} = CSR^*_{Eq} \quad ...(2.38)$$

where,

$$K_\sigma = (\sigma'_v)^{f-1} \quad ...(2.39)$$

σ'_v = Effective overburden stress in kg/cm^2.

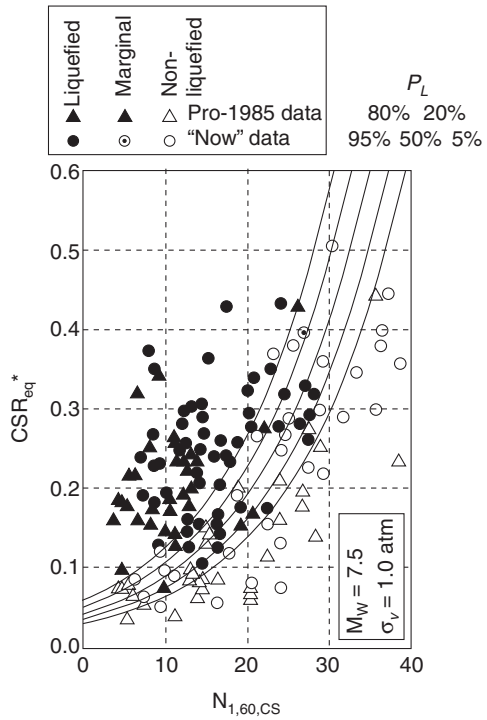

Fig. 2.24 Recommended probabilistic standard penetration test-based liquefaction triggering correlation for M_w = 7.5 and σ_v = 1.0 atm (after Cetin, 2004).

ILLUSTRATIVE EXAMPLES

Example 2.1 A 200 mm high specimen of clayey sand with a unit weight of 18.0 kN/m^3 is tested in a resonant column device having weight of specimen to weight of loading system ratio as 0.3 and ratio of mass polar moment of inertia of the specimen to mass polar moment of inertia torsional loading system as 0.22. When the column is excited longitudinally, the frequency-response curve as shown in Fig. 2.25(a) was obtained. Figure 2.25(b) shows the frequency-response curve when the column was excited torsionally. Determine the Young's modulus, shear modulus and Poisson's ratio of the soil.

Solution From Fig. 2.25(a), the fundamental frequency f_{nl} of the specimen vibrating longitudinally is 35 cps. The Eq. (2.1) may be written as,

$$\frac{W}{W_o} = \frac{\omega_{nl} h}{V_l} \tan\left(\frac{\omega_{nl} h}{V_l}\right) = 0.3$$

Solving the above equation by trial, we get,

$$\frac{\omega_{nl} h}{V_l} = 0.52$$

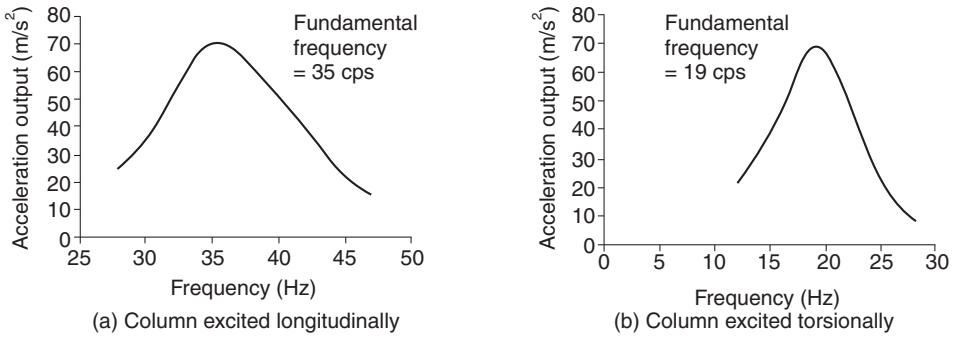

Fig. 2.25 Acceleration-frequency response curves for resonant column test

or,
$$V_l = \frac{2\pi \times 35 \times 0.2}{0.52} = 84.54 \text{ m/s}$$

From Eq (2.3),

$$E = \rho V_l^2 = \frac{\gamma}{g} V_l^2$$

or,

$$E = \frac{18}{9.89} 84.54^2 = 13.08 \times 10^3 \text{ kN/m}^2$$

From Fig. 2.25(b), the fundamental frequency f_{ns} of the specimen vibrating torsionally is 19 cps. Eq. (2.5) may be written as,

$$\frac{I}{I_o} = \frac{\omega_{ns} h}{V_s} \tan\left(\frac{\omega_{ns} h}{V_s}\right) = 0.22$$

Solving the above equation by trial, we get,

$$\frac{\omega_{ns} h}{V_s} = 0.45$$

or,
$$V_s = \frac{2\pi \times 19 \times 0.2}{0.45} = 84.54 \text{ m/s}$$

From Eq. (2.7),

$$G = \rho V_s^2 = \frac{\gamma}{g} V_s^2$$
$$= \frac{18}{9.81} \times 53.03^2 = 5.16 \times 10^3 \text{ kN/m}^2$$

As,

$$G = \frac{E}{2(1 + \mu)}$$

$$\mu = \frac{E}{2G} - 1 = \frac{13.08 \times 10^3}{2 \times 5.16 \times 10^3} - 1 = 0.267$$

Table 2.5 Analysis of cyclic plate load test data

Sr. No.	*Pressure (kN/m²)*	*Settlement (mm)*				*Average*	*Average elastic*
		Gauge No. 1	*Gauge No. 2*	*Gauge No. 3*	*Gauge No. 4*	*settlement (mm)*	*settlement (mm)*
(1)	*(2)*	*(3)*	*(4)*	*(5)*	*(6)*	*(7)*	*(8)*
1.	0	0	0	0	0	0	
2.	25	0.38	0.50	0.04	0.43	0.3375	0.1150
3.	0	0.31	0.34	–0.04	0.28	0.2225	
4.	50	1.00	1.17	0.65	1.03	0.9625	0.2725
5.	0	0.73	0.85	0.40	0.78	0.6900	
6.	75	2.06	1.97	1.42	2.03	1.8700	0.5475
7.	0	1.48	1.45	0.98	1.38	1.3225	
8.	100	2.86	2.47	1.92	2.90	2.5375	0.7075
9.	0	2.01	1.86	1.42	2.03	1.8300	
10.	125	3.41	2.97	2.30	3.58	3.0650	0.7750
11.	0	2.56	2.35	1.68	2.57	2.2900	
12.	150	4.18	3.86	2.82	4.32	3.7950	1.4675
13.	0	3.16	2.92	2.02	1.21	2.3275	
14.	175	5.16	4.65	3.52	5.20	4.6325	1.1875
15.	0	3.76	3.47	2.55	4.00	3.4450	
16.	200	6.28	5.47	4.10	6.13	5.4950	1.1500
17.	0	5.38	4.07	2.95	4.98	4.3450	
18.	225	8.06	6.32	4.35	7.38	6.5275	1.2500
19.	0	6.74	4.92	3.22	6.23	5.2775	
20.	250	10.35	8.17	6.35	9.33	8.5500	2.0400
21.	0	8.84	5.79	4.03	7.38	6.5100	
22.	275	12.14	10.24	8.56	9.49	10.1075	2.2225
23.	0	9.74	8.54	5.86	7.40	7.8850	
24.	300	13.45	11.87	11.22	10.38	11.7300	1.1275
25.	0	11.56	10.67	10.30	9.88	10.6025	

$$\overline{\sigma}_{01} = (\overline{\sigma}_{v1} + \overline{\sigma}_{v2})\frac{(1 + 2K_0)}{3}$$

$$K_0 = 0.4 \text{ (given)}$$

Pressure intensity below the actual footing (3.0 m × 3.0 m having base at a depth equal to 2.0 m below ground surface).

$$\overline{\sigma}_{v1a} = 17 \times (2.0 + 3.0) = 85.00 \text{ kN/m}^2$$

$$m = \frac{L/2}{Z} = \frac{3.0/2}{3.0} = 0.5$$

$$n = \frac{B/2}{Z} = \frac{3.0/2}{3.0} = 0.5$$

$$q = 24 \times 1.50 = 36.0 \text{ kN/m}^2$$

[assuming unit weight of concrete = 24 kN/m^3]

$$\overline{\sigma}_{v2a} = 0.3362 \times 36 = 12.10 \text{ kN/m}^2$$

$$\overline{\sigma}_{02} = (\overline{\sigma}_{v1a} + \overline{\sigma}_{v2a})\frac{(1 + 2K_0)}{3} = (85 + 12.10)\frac{(1 + 2 \times 0.4)}{3}$$

$$= 58.26 \text{ kN/m}^2$$

Correction to the values of E can be applied as given below

$$E_c = \left(\frac{\overline{\sigma}_{02}}{\overline{\sigma}_{01}}\right)^{0.5} E$$

Table 2.6 Confining pressure correction to elasrtic modulus

Pressure intensity (kN/m^2)	*$\overline{\sigma}_{v2}$ (kN/m^2)*	*$\overline{\sigma}_{01}$ (kN/m^2)*	*Corrected elastic modulus, E_c (kN/m^2)*	*Strain level ×10^{-3}*
50	16.81	33.55	53.53	0.91
150	50.43	53.72	42.43	2.36
200	67.24	63.30	38.81	3.83
250	84.05	73.89	36.07	6.80

$$\text{Permissible strain level} = \frac{\text{Permissible amplitude}}{\text{Width of actual block}} = \frac{5}{3000} = 1.667 \times 10^{-3}$$

By interpolation (Table 2.6) gives the value of elastic modulus as 47.74 kN/m^2 for the strain level of 1.667×10^{-3}. This value of E may be adopted for the analysis and design of actual foundation.

Example 2.3 A vertical block vibration was conducted on 1.5 m × 0.75 m × 0.75 m high concrete block in an open pit having depth of 1.5 m which is equal to the anticipated depth of actual foundation. The test was repeated at different settings (θ) of eccentric masses.

where,

$\overline{\sigma}_v = \overline{\sigma}_{v1} + \overline{\sigma}_{v2}$,

$\overline{\sigma}_{v1}$ = effective overburden pressure at the depth under consideration, and

$\overline{\sigma}_{v2}$ = increase in vertical pressure due to weight of block.

Assuming that top 2.0 m soil has a moist unit weight of 18 kN/m^3 and saturated unit weight below water table is 20 kN/m^3, then

$$\overline{\sigma}_{v1} = 18 \times 2.0 + 10 \times \frac{0.25}{2} = 37.25 \text{ kN/m}^2$$

From Taylor (1948):

$$\overline{\sigma}_{v2} = \frac{4q}{4\pi}\left[\frac{2mn\sqrt{m^2+n^2+1}}{m^2+n^2+1+m^2n^2}\,\frac{m^2+n^2+2}{m^2+n^2+1} + \sin^{-1}\frac{2mn\sqrt{m^2+n^2+1}}{m^2+n^2+1+m^2n^2}\right]$$

$$m = \frac{L/2}{Z} = \frac{1.5/2}{0.75} = 1.0$$

$$n = \frac{L/2}{Z} = \frac{0.75/2}{0.75} = 0.5$$

$$q = 24 \times 0.75 = 18.0 \text{ kN/m}^2$$

[assuming unit weight of concrete = 24 kN/m^3]

Substituting the above values of m, n, and q in the expression of $\overline{\sigma}_{v2}$, we get

$$\overline{\sigma}_{v2} = 0.4808q = 8.65 \text{ kN/m}^2$$

$$\overline{\sigma}_v = 37.25 + 8.65 = 45.90 \text{ kN/m}^2$$

$$k_0 = 1 - \sin\phi = 1 - \sin 30° = 0.5$$

$$\overline{\sigma}_{01} = 45.90\,\frac{(1 + 2 \times 0.5)}{3} = 30.60 \text{ kN/m}^2$$

For the actual foundation

$$\overline{\sigma}_{v1} = 18 \times 2.0 + 10 \times 2.5 = 61.0 \text{ kN/m}^2$$

$$m = \frac{4.0/2}{3.0} = 0.67$$

$$n = \frac{3.0/2}{3.0} = 0.50$$

$$q = 24 \times 1.0 = 24.0 \text{ kN/m}^2$$

[assuming unit weight of concrete = 24 kN/m^3]

Substituting the above values of m, n, and q in the expression of $\overline{\sigma}_{v2}$, we get

$$\overline{\sigma}_{v2} = 0.4035q = 9.68 \text{ kN/m}^2$$

$$\overline{\sigma}_v = 61.0 + 9.68 = 70.68 \text{ kN/m}^2$$

$$\bar{\sigma}_{02} = 70.68 \left(\frac{1 + 2 \times 0.5}{3}\right) = 47.11 \text{ kN/m}^2$$

$$\frac{E_1}{E_2} = \frac{G_1}{G_2} = \left(\frac{\bar{\sigma}_{02}}{\bar{\sigma}_{01}}\right)^{0.5} = \left(\frac{47.11}{30.60}\right)^{0.5} = 1.24$$

The values of E and G of the actual foundation at different strain levels (= amplitude at resonance/width of the block) are given in Cols. 8 and 9 of Table 2.7 respectively. The corresponding values are listed in Col. 11.

4. Strain level correction

Desired strain level

$$= \frac{150 \times 10^{-6}}{3} = 0.5 \times 10^{-4}$$

$$E = 8.98 \times 10^4 - \frac{(8.98 \times 10^4 - 6.93 \times 10^4)}{(0.51 - 0.40)} (0.5 - 0.4)$$

$$= 7.12 \times 10^4 \text{ kN/m}^2$$

$$G = 3.46 \times 10^4 - \frac{(3.46 \times 10^4 - 2.67 \times 10^4)}{(0.51 - 0.40)} (0.5 - 0.4)$$

$$= 2.74 \times 10^4 \text{ kN/m}^2$$

Example 2.4 A cross borehole test was carried out at a site using three boreholes having centre to centre spacing of 6.0 m. The depth of each borehole was 15.0 m. The aim was to obtain shear wave velocity profile upto a depth of 12.5 m performing tests at 2.5 m depth interval. The first borehole was used as the source, while other two for recording travel times through geophones. Following observations were obtained during the test:

Depth (m)	*Travel time T_{s1} (milli seconds) (S_1 = 6.0 m)*	*Travel time T_{s2} (milli seconds) (S_2 = 12.0 m)*
2.5	53	102
5.0	56	107
7.5	75	155
10.0	78	170
12.5	45	92

Solution Shear wave velocities (V_s) will be as given below:

Depth (m)	*V_{s1} (m/s^2)*	*V_{s2} (m/s^2)*	*Average velocity V_s (m/s^2)*	*Shear modulus (G) (kN/m^2)*
2.5	113.2	117.6	115.4	2.40 x 10^4
5	107.1	112.1	109.6	2.16 x 10^4
7.5	80.0	77.4	78.7	1.12 x 10^4
10	76.9	70.6	73.8	1.00 x 10^4
12.5	133.3	130.4	131.8	3.13 x 10^4

The values of shear modulus G are obtained using Eq. 2.7, assuming unit weight of soil as 18.0 kN/m^2.

Table 2.7 Analysis of vertical block vibration test data for C_u, E and G

Sr. No.	θ (deg)	f_{nz}	Amplitude at resonance (microns)	For test block			For actual foundation		Strain level × 10^{-4}
				C_u × 10^4 kN/m^2	E × 10^4 kN/m^2	G × 10^4 kN/m^2	E × 10^4 kN/m^3	G × 10^4 kN/m^2	
(1)	(2)	(3)	(4)	(5)	(6)	(7)	(8)	(9)	(10)
1.	24	40	12	12.49	10.96	4.22	13.59	5.23	0.16
2.	48	37	22	10.69	9.38	3.61	11.63	4.47	0.29
3.	72	33	30	8.50	7.46	2.87	9.25	3.56	0.40
4.	96	29	38	6.57	5.76	2.22	7.14	2.75	0.51

Table 2.8 Details of computations for obtaining liquefaction potential by Seed and Idriss (1971) method

Sr. No.	*Depth (m)*	*Total stress (kN/m^2)*	r_d	τ_{av} (kN/m^2)	*Effective stress (kN/m^2)*	D_R (%)	C_r	$\sigma_d/2\sigma_3$	τ_h (kN/m^2)	τ_{av}/τ_h
1.	1.5	27	0.99	2.26	27	22	0.550	0.228	1.49	1.52
2.	3.0	57	0.98	4.72	42	30	0.550	0.23	3.19	1.48
3.	4.5	87	0.97	7.14	57	33	0.550	0.215	4.45	1.60
4.	6.0	117	0.97	9.60	72	38	0.550	0.22	6.62	1.45
5.	7.5	147	0.96	11.93	87	45	0.555	0.217	9.43	1.27
6.	9.0	177	0.95	14.22	102	50	0.570	0.223	12.97	1.10
7.	10.5	207	0.94	16.46	117	48	0.560	0.23	14.47	1.14
8.	12.0	237	0.92	18.44	132	45	0.556	0.232	15.32	1.20
9.	13.5	267	0.91	20.55	147	58	0.576	0.232	22.79	0.90
10.	15.0	297	0.9	22.61	162	62	0.608	0.235	28.70	0.79

(b) Seed (1979) method

(i) In this method, the value of shear stress at any depth included by the earthquake is obtained exactly in the same manner as illustrated in Seed and Idriss (1971) method.

(ii) To determine τ_h value firstly *N*-values are corrected for effective overburden pressure using Fig. 2.16. The stress ratio τ_h/σ'_v is then obtained using interpolation from Fig. 2.18 for the given value of corrected *N*. The details of computations are given in Table 2.9.

Table 2.9 Details of computations for obtaining liquefaction potential by Seed (1979) method

Sr. No.	*Depth (m)*	*Effective stress (kN/m^2)*	*N-Value*	*Corrected N-Value*	τ_h/σ'_v	τ_h (kN/m^2)	τ_{av}/τ_h
1.	1.5	27	4	6	0.07	1.89	1.20
2.	3.0	42	6	8	0.085	3.57	1.32
3.	4.5	57	8	10	0.115	6.555	1.09
4.	6.0	72	10	11	0.12	8.64	1.11
5.	7.5	87	15	16	0.185	16.095	0.74
6.	9.0	102	18	18	0.2	20.4	0.70
7.	10.5	117	22	21	0.245	28.665	0.57
8.	12.0	132	20	18	0.2	26.4	0.70
9.	13.5	147	25	22	0.255	37.485	0.55
10.	15.0	162	28	24	0.31	50.22	0.45

(c) Iwasaki (1986) method

(i) Firstly the values of factor *R* are obtained using the following expression,

$$R = 0.882 \sqrt{\frac{N}{\bar{\sigma}_v + 70}} + 0.225 \log_{10}\left(\frac{0.35}{D_{50}}\right)$$

(ii) The factor *L* is then obtained using the following expression,

$$L = \frac{a_{\max}}{g} \frac{\sigma_v}{\bar{\sigma}_v} r_d$$

The details of computations are given in Table 2.10. The values of factor of safety F_L are listed in the last column of Table 2.10.

Table 2.10 Details of computations for obtaining liquefaction potential by Iwasaki (1986) method

Sr. No.	*Depth (m)*	D_{50} *(mm)*	*Total stress (kN/m^2)*	*Effective stress (kN/m^2)*	*R*	r_d	*L*	F_L
1.	1.5	0.18	27	27	0.24409	0.9775	0.12718	1.91
2.	3.0	0.2	57	42	0.25883	0.955	0.16863	1.53
3.	4.5	0.12	87	57	0.32597	0.9325	0.18518	1.76
4.	6.0	0.14	117	72	0.32359	0.91	0.19239	1.68
5.	7.5	0.13	147	87	0.3694	0.8875	0.1951	1.89
6.	9.0	0.16	177	102	0.36181	0.865	0.19529	1.85
7.	10.5	0.2	207	117	0.35721	0.8425	0.19393	1.84

Table 2.10 contd..

$$C_{\text{fines}} = (1 + 0.004 \times 8) + 0.05 \left(\frac{8}{15.48}\right)$$

$$= 1.032 + 0.0258 = 1.0578$$

$$N_{1,60CS} = 1.0578 \times 15.48 = 16.37 \approx 16$$

2. $$\text{CSR}_{\text{Eq}} = 0.65 \left(\frac{a_{\max}}{g}\right) \left(\frac{\sigma_v}{\sigma'_v}\right) r_d$$

From Fig. 2.21, $r_d = 0.88$

$$\text{CSR}_{\text{Eq}} = 0.65 \left(\frac{0.15g}{g}\right) \left(\frac{18 \times 2.0 + 20 \times 3.0}{66}\right) 0.88$$

$$\text{CSR}_{\text{Eq}} = 0.1248$$

3. For $Mw = 6.5$, Fig. 2.22 gives $\text{DWF}_{\text{M}} = 1.25$,

$$\text{CSR}_{\text{Eq},M=7.5} = \frac{\text{CSR}_{\text{Eq}}}{\text{DWF}_{\text{M}}} = \frac{0.1248}{1.25} = 0.0998$$

$$\text{CSR*}_{\text{Eq}} = \frac{\text{CSR}_{\text{Eq, } M = 7.5}}{K_\sigma}$$

For $D_r = 40$ % and $\sigma'_{\text{v}} = 66$ kN/m^2, Fig. 2.23 gives the value of K_σ as 1.18

$$\text{CSR*}_{\text{Eq}} = \frac{0.0998}{1.18} = 0.0846$$

For $N_{1,60CS} = 16$ and $\text{CSR*}_{\text{Eq}} = 0.0846$, Fig. 2.24 gives $P_L = 5\%$

Therefore, in the strata given in the problem, there is 5% probability of initiation of liquefaction at a depth equal to 5.0 m below ground surface.

REFERENCES

Anderson, D.G. (1974), "Dynamic modulus of cohesive soils", Ph.D. Dissertation, University of Michigan, Ann Arbor.

Casagrande, A. (1965), "The role of the calculated risk in earthwork and foundation engineering", J. Soil mech. and Found. Div., ASCE, 91(SM-4), pp. 1-40, Proc. Paper. 4390.

Cetin, K. O., Seed R. B., Kiureghian, A. D., Tokimatsu, K., Harder, L. F. Jr., Kayen, R. E., and Moss, R. E. S. (2004), Journal of Geotechnical and Geoenvironmental Engineering, Vol. 130(12), pp. 1314-1340.

Corps of Engineers, U.S. Department of the army (1939), "Report of the slide of a portion of upstream face at fort peck dam", U.S. Government Printing Press, Washington, D.S.

Drnevich, V.P. (1967), "Effect of strain history on the dynamic properties of sand", Ph.D. Dissertation, University of Michigan, Ann Arbor.

Drnevich, V.P. (1972), "Undrained cyclic shear of saturated sand", J. Soil mech. and Found. Div., ASCE, 38(SM-8), pp. 807-825.

Seed, H. B. (1979)' "Soil liquefaction and cyclic mobility for level ground during earthquakes", J. Geotech Eng. Div., ASCE, 10(GT-2), pp. 201-255.

Teraghi, K. L., and Peck, R. B. (1967), "Soil mechanics in engineering practice", John Wiley and Sons Inc., New York.

Waterways Experiments Station, U. S. Corps of Engineers (1967), "Potamology investigation, report 12-18, verification of empirical method for determining river bank stability", 1965 Data, Vicksburg, Mississippi.

Woods, R.D. (1978), "Measurement of dynamic soil properties: state-of-the-art", Proc. ASCE Spec. conf. Earthquake Eng. Soil Dyn., Pasadena, CA, Vol. 1, pp. 91-180.

Youd, T. L., et al. (2001). "Liquefaction resistance of soils; summary report from the 1996 NCEER and 1998 NCEER/NSF workshops on evaluation of liquefaction resistance of soils." J. Geotech. Geoenviron. Eng., 127(10), 817–833.

PRACTICE PROBLEMS

1. Explain stepwise procedure of obtaining elastic and shear modulii (E and G) using resonant column apparatus. Illustrate your answer with neat sketches.
2. Give salient features of the cyclic plate load test and vertical block resonant test for obtaining elastic modulus of soil (E). What are the approximate values of strain levels associated with these tests?
3. Write short notes on:
   (a) Cross-borehole test
   (b) SASW test
4. Explain the basic mechanism of liquefaction. What are the factors affecting liquefaction?
5. Give stepwise the procedure for obtaining the probability of initiation of liquefaction.
6. A 200 mm high specimen of clayey sand with a unit weight of 17.5 kN/m^3 is tested in a resonant column device having weight of specimen to weight of loading system ratio as 0.275 and ratio of mass polar moment of inertia of the specimen to mass polar moment of inertia torsional loading system as 0.25. The fundamental frequencies were observed to be 40 cps and 22 cps in cases when column is excited longitudinally and for the column excited torsionally respectively. Determine the Young's modulus, shear modulus and Poisson's ratio of the soil.
7. A cyclic plate load test was performed at a site having silty sand upto 9 m depth. The test was performed on a square plate of size 450 mm × 450 mm in a pit of size 2.25 m × 2.25 m × 3.0 m deep. The data obtained from the test was as given in following table. The water table was below 8.0 m depth. Assume the value of the coefficient of earth pressure at rest as 0.4 and unit weight of soil as 18.0 kN/m^3.

adopted for the design of actual foundation. Limiting vertical amplitude of machine is 100 microns. Assume Poisson's ratio as 0.3.

9. At a given site, a boring supplemented with standard penetration tests was done up to 12.0 m depth. The results of the boring are as given below.

Depth (m)	*Classification of soils*	*D_{50} (mm)*	*N-Value*	*D_R (%)*	*Remarks*
1.5	SP	0.18	3	19	(a) Position of water table lies 3.0 m below
3.0	SP	0.2	6	30	the ground level.
4.5	SM	0.12	8	33	
6.0	SM	0.14	10	38	(b) γ_{moist} = 17 kN/m^2
7.5	SM	0.13	15	45	γ_{sub} = 10 kN/m^2
9.0	SP	0.16	18	52	
10.5	SW	0.20	22	50	
12.0	SW	0.22	20	46	

The site is located in seismically active region, and is likely to be subjected by an earthquake of magnitude 8.0. Determine the zone of liquefaction using:

(i) Seed and Idriss (1971) method

(ii) Seed (1979) method

(iii) Iwasaki (1986) method

Also determine probability of initiation of liquefaction at the depth of 7.5 m and 10.5 m, if the fine contents at these depths are 7% and 5% respectively.